ARTICLE

Low-Temperature, Highly Efficient Growth of Carbon Nanotubes on Functional Materials by an Oxidative Dehydrogenation Reaction

Arnaud Magrez,[†,‡,*] Jin Won Seo,[§] Rita Smajda,[†] Barbara Korbely,[⊥] Juan Carlos Andresen,[†] Marijana Mionić,[†] Stéphane Casimirius,[†] and László Forró[†]

[†]Laboratoire de Physique de la Matière Complexe, Ecole Polytechnique Fédérale de Lausanne, Switzerland, [‡]Center for Research on Electronically Advanced Matter, Ecole Polytechnique Fédérale de Lausanne, Switzerland, [§]Department Metallurgy and Materials Engineering, Katholieke Universiteit Leuven, Belgium, and [⊥]Department of Applied and Environmental Chemistry, University of Szeged, Hungary

ABSTRACT In many applications like photovoltaics, fuel cells, batteries, or interconnects in integrated circuits carbon nanotubes (CNTs) have the role of charge transport electrodes. The building of such devices requires an *in situ* growth of CNTs at temperatures where the structure or chemical composition of the functional materials is unaltered. We report that in a chemical vapor deposition process involving an oxidative dehydrogenation reaction of C_2H_2 with CO_2 growth temperatures below 400 °C are achieved. Furthermore, the growth can be performed on versatile materials ranging from metals through oxides to organic materials.

KEYWORDS: carbon nanotubes · oxidative dehydrogenation · acetylene · CO_2 · chemical vapor deposition

The ability to grow carbon nanotubes (CNTs) on all sorts of materials is one of the key issues for the effective integration of CNTs in numerous applications with their existing process flows. Using chemical vapor deposition (CVD), which involves the catalytic decomposition of a carbon containing gas over a supported catalyst, the growth of CNTs has been achieved on several support materials with controlled characteristics, such as diameter, length, and number of walls.[1−3] However, successful CNT synthesis relies mostly on empirical basis: each growth parameter, for instance, a proper selection of carbon-containing precursor compound, catalyst material, growth temperature, residence time in the reaction zone, and gas flow conditions require optimization. In particular, the interaction between the catalyst particle and the support strongly affects the CNT growth,[4−6] and the best synthetic parameters are in general specific for each support material. On several materials the CNT growth has been elusive. For instance, on Si and metals, the spontaneous formation of silicides and metallic alloys respectively poisons the catalyst and dramatically reduces the catalytic efficiency. Therefore, oxides (*e.g.*, Al_2O_3, SiO_2, MgO), nitrides, or highly stable metals, such as Ta, have been the most favored support materials.[7,8]

Recent breakthrough in the growth of CNTs have demonstrated that large scale and ultrahigh yield growth of vertical CNT forest could be obtained by adding oxygen containing species, together with the carbon source.[9−12] This highly efficient growth has been explained by the fact that the presence of weak oxidizer preserves the catalytic activity by etching the amorphous carbon coating. However, the amount of oxidizer is extremely low, hardly controllable, and appears to strongly depend on the synthesis setup. So far, enormous variations of the optimum oxidizer content have been reported.[9−15] Nitrogen containing species have also proven to enhance the CNTs growth. However, the yield of CNTs growth remains low as compared to processes using oxygen containing species.[16]

Here, we report a flexible and highly reproducible synthetic approach for the synthesis of CNTs using an oxidative dehydrogenation reaction of acetylene. Actually, catalytic reactions based on oxidative dehydrogenation are widely used processes in olefin industry for the production of unsaturated hydrocarbons.[17] However, to our knowledge it has never been considered for the synthesis of CNTs. We have discovered that the oxidative dehydrogenation of C_2H_2 with CO_2 improves the CNTs growth efficiency drastically. The activity and the

*Address correspondence to arnaud.magrez@epfl.ch.

Received for review February 10, 2010 and accepted June 7, 2010.

Published online June 17, 2010. 10.1021/nn100279j

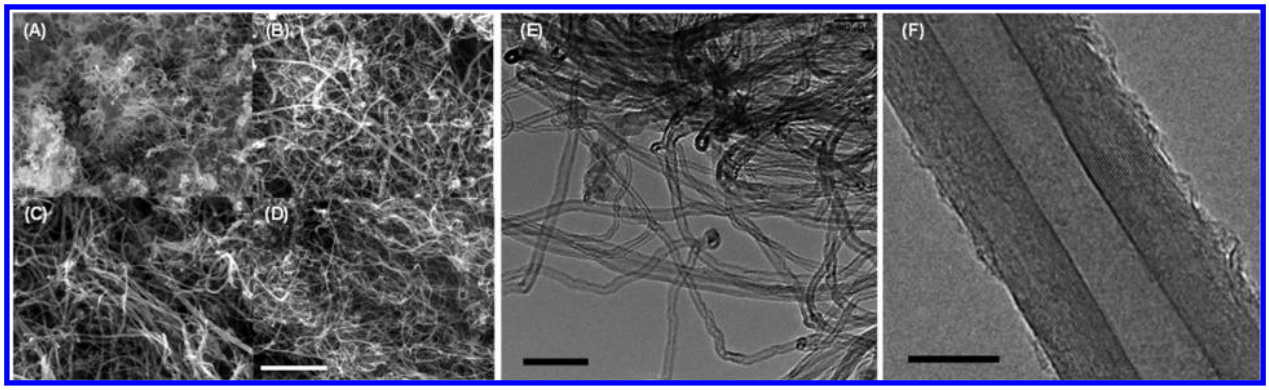

Figure 1. CNTs grown by the oxidative dehydrogenation reaction of C_2H_2 with CO_2. Scanning electron micrographs of CNTs grown on Fe_2Co alloy supported by boride (A), nitride (B), carbide (C), and oxide (D) materials (scale bar is 1 μm). (E) Representative low-magnification TEM image of CNTs. Scale bar is 50 nm. (F) High resolution TEM image of a nanotube. Scale bar is 10 nm.

lifetime of the catalyst is enhanced to such an extent that it allows CNT growth at temperatures below 400 °C without any arduous activation of the catalyst prior to the growth. Moreover, the growth can be performed on numerous functional materials, nonconventional substrates such as bulk Cu, organic materials, carbon, glass, and most ceramics. This opens new avenues for integration of CNTs in functional devices.

Figure 1 demonstrates representative growth of CNTs produced by the oxidative dehydrogenation reaction of C_2H_2 with CO_2 on a broad range of support materials including oxides, borides, carbides, and nitrides (Figure 1A−D). The particles of these materials are decorated prior to the growth with Fe-based metallic nanoparticles by a simple coprecipitation process. X-ray powder diffraction before and after the CNT growth reveals that support materials do not experience any significant chemical or structural modification (Supporting Information Figure S1). At the end of the CNTs synthesis, support particles are homogeneously covered with CNTs. Their density on the support surface as well as their diameter can easily be controlled by the distribution and the size of the metallic particles coating the support surface.

Produced materials contain large quantities of CNTs with C/support and C/metal ratios as high as 10000 mol % and 150000 at % (Figure 2), respectively.[18] The highest C/metal ratio obtained with the oxidative dehydrogenation reaction is close to the best yields obtained with the CVD process assisted by oxygen-containing species.[9] The form of carbon deposited strongly depends on the C_2H_2/CO_2 ratio. In the case of an equimolar stoichiometry between C_2H_2 and CO_2, the carbon phase produced is entirely composed of CNTs.[19] As transmission electron microscopy (TEM) images indicate (Figure 1E,F), CNTs are multiwalled, of high crystallinity, and free of amorphous carbon. The walls are clean and parallel. Similar structural characteristics are found in all samples independent of the substrate material used (Supporting Information Figure S2).

For the oxidative dehydrogenation reaction, two overall chemical mechanisms are proposed and described by the following equations:

$$C_2H_2 + CO_2 \rightarrow 2C + H_2O + CO \quad (1)$$

$$C_2H_2 + CO_2 \rightarrow C + 2CO + H_2 \quad (2)$$

Besides the competition between these two mechanisms, the classical route of thermal decomposition of acetylene can occur. However, the decomposition is kinetically limited at low temperatures. While amorphous carbon is deposited, no nanotubes are produced by the acetylene decomposition with our experimental settings at temperatures below 600 °C. Gibbs energy calculations indicate that both reactions between C_2H_2 and CO_2 proposed above are spontaneous despite that reaction 1 is thermodynamically preferred below 640 °C (Supporting Information Figure S3). To identify the precise chemical mechanism involved in the CNTs growth, we performed residual gas composition analysis at the exhaust during the synthesis by means of quadrupolar mass spectrometry. Particularly, the evolution of the partial pressure of the main reaction products, namely water (H_2O) and carbon monoxide (CO), was carefully studied as a function of time and growth temperature.

Figure 3 summarizes the synthesis of CNTs catalyzed by Fe_2Co supported by Nb_2O_5, which is used as

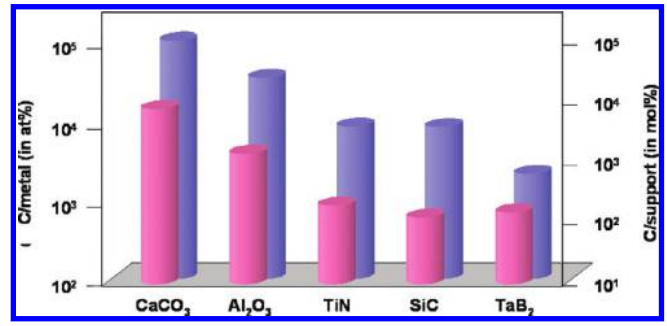

Figure 2. Histograms of the C/metal (blue) and C/support (pink) ratios for carbonate, borides, nitrides, oxides, carbides materials. The oxidative dehydrogenation reaction is a very high yield process similar to the water-assisted method for which C/metal is about 1.9×10^5 atom % (ref 9).

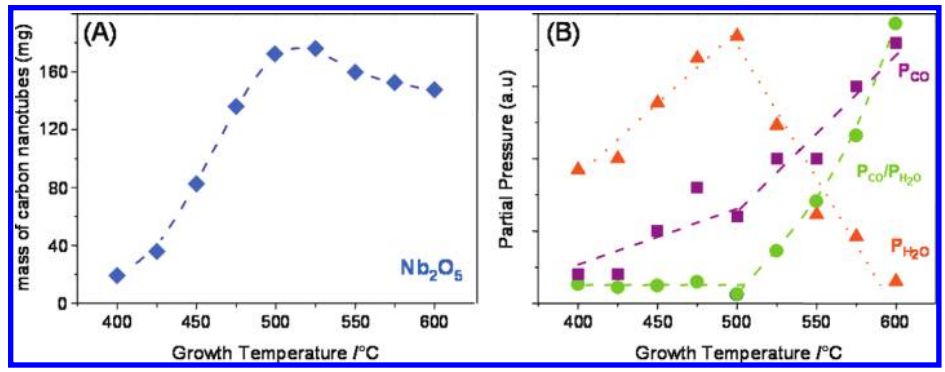

Figure 3. Mass of CNTs produced (from 400 to 600 °C) over 500 mg of Fe_2Co supported by Nb_2O_5 as a function of growth temperature (A). Maximum water and CO partial pressure produced and ratio between the maximum CO and water partial pressures as a function of growth temperature (B).

our model system. Nb_2O_5, used in electrochromic and photovoltaic applications,[20] exhibits very high chemical stability under the applied CNT growth conditions. Using Nb_2O_5, a large amount of CNTs can be grown below 600 °C (Supporting Information Figure S4) while Nb_2O_5 particle size remains constant. Hence, metal nanoparticles' coarsening is avoided during the growth of nanotubes. As illustrated in Figure 3A, the quantity of CNTs produced significantly depends on the growth temperature applied with a maximum yield at around 500 °C. The amount of water (ΔP_{H_2O}) and carbon monoxide (ΔP_{CO}) produced during the synthesis undergo a similar growth temperature dependence (Figure 3B). As water exclusively exhausts in the reaction 1, the chemical mechanism involved in the synthesis of CNTs can be identified by tracing its amount. As shown in Figure 3A, when the temperature is raised from 400 to 500 °C, kinetics of the CNTs synthesis is thermally enhanced: the mass of CNTs increases along with the amount of water and carbon monoxide produced. In this regime the ratio $\Delta P_{CO}/\Delta P_{H_2O}$ remains constant (see Figure 3B). This is in agreement with the oxidative dehydrogenation reaction of C_2H_2 with CO_2 described by eq 1 where H_2O is produced in equal proportion to CO. At 500 °C, an abrupt transition of the CNT yield, the ΔP_{H_2O} and the ΔP_{CO} occurs. The ratio $\Delta P_{CO}/\Delta P_{H_2O}$ starts to increase dramatically. This significant change in the reaction gas composition at 500 °C is a result of a progressive shift in the chemical reaction path. In particular, it is the result of a constant decrease of the partial pressure of H_2O produced while the CO production accelerates (Figure 3B). The decrease of ΔP_{H_2O} as well as the increase of ΔP_{CO} is ascribed to stoichiometry differences in the reaction products: in the reaction 1, one molecule of CO and H_2O are produced per C_2H_2 molecule, whereas reaction 2 leads to two CO molecules per C_2H_2 molecule without any H_2O molecules. The transition from the reaction path (1) to reaction path (2) also explains the slight decrease in the mass of resulting nanotubes above 500 °C: despite the thermal enhancement of the reaction kinetic, twice less C atoms are produced per C_2H_2 molecule along reaction 2 compared to that produced along reaction 1. These results clearly demonstrate that the oxidative dehydrogenation reaction of C_2H_2 with CO_2 proceeds along reaction 1 below 500 °C, whereas the reaction 2 is kinetically preferred above 500 °C.

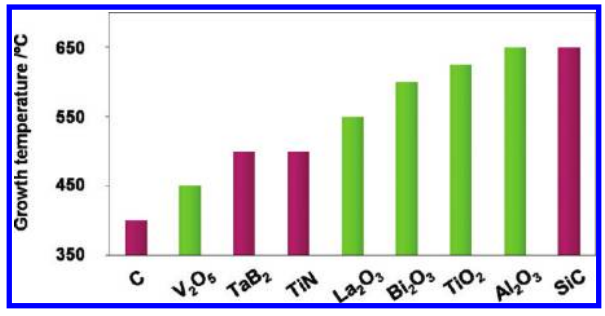

Figure 4. Catalyst support dependence of the temperature of maximum yield for the oxidative dehydrogenation reaction over catalyst supported by oxide (green) and non-oxide (purple) substrates.

It has to be noted that the oxidative dehydrogenation reaction of C_2H_2 with CO_2 enhances the CNT growth kinetics and reduces the growth temperature to such an extent that the catalyst poisoning by the underlying support is suppressed. We take full advantage of this fact to grow CNTs at low temperatures on many functional substrates including oxides and nonoxide materials (Figure 4). On all these substrate materials, CNTs have been successfully grown with at least 10 times higher yield than with the conventional acetylene decomposition (Figure 2). Figure 4 shows that the temperature of maximum yield is support specific: it varies from 400 to 650 °C for nine different support materials, namely V_2O_5, TiO_2, Bi_2O_3, La_2O_3, Al_2O_3, MgO, C, TiN, TaB_2, and SiC. This dependence has to be attributed *de novo* to the change in the chemical mechanism of the oxidative dehydrogenation reaction. We believe that the variation in the maximum yield temperature is due to the difference in adsorption strength and configurations of the gas molecules on the surface of the supported catalyst. At early stages, C_2H_2 molecules adsorb most likely on the metal surface while CO_2 adsorption preferentially occurs on the support to form carbonate-like surface adsorbate.[21] The oxidative dehy-

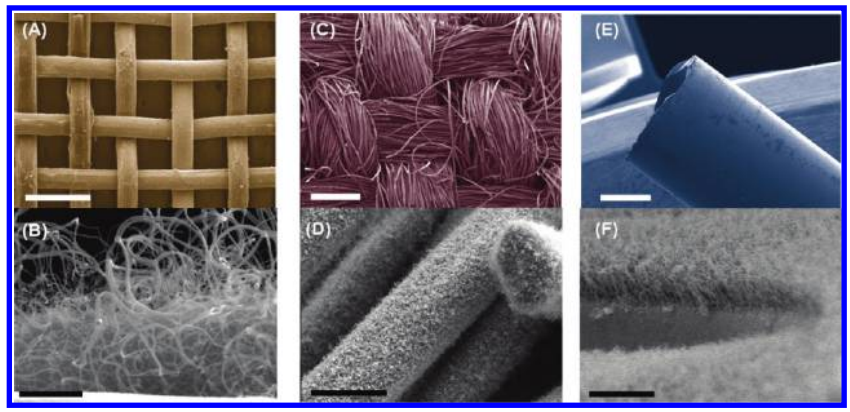

Figure 5. Growth of CNTs by the oxidative dehydrogenation reaction of C_2H_2 with CO_2, at 600 °C, on substrates with various forms. All three materials were coated with catalyst by evaporating 5 nm Fe film: copper mesh, scale bar is (A) 500 μm and (B) 2 μm; carbon fiber textile, scale bar is (C) 500 μm and (D) 20 μm; rim of a Pasteur pipet, scale bars are (E) 500 μm and (F) 2 μm.

drogenation reactions could proceed subsequently at the triple-point junction, which lies around the interface between the metal particle and the support of the catalyst. The CNT formation is confined to this area where C_2H_2 and CO_2 adsorb. The hypothesis of CNT growth to possibly stem from the support is corroborated by recent TEM observations of CNTs anchored onto oxide supports in the presence of metal nanoparticles.[22]

It has to be emphasized that the oxidative dehydrogenation reaction of C_2H_2 with CO_2 allows us to vary the optimum CNT growth temperature in a broad window of 400 °C up to 650 °C by selecting the appropriate support material with the characteristic optimum CNT growth temperature (Figure 4). One additional valuable advantage of the oxidative dehydrogenation reaction is that the end product exclusively consists of CNTs even at non-optimum growth temperature (optimum growth temperature ±100 °C) but with reduced yield. Hence, the total applicable growth temperature range sums up to 300−750 °C. Moreover, other classes of substrate materials may exist, which have not yet been included in this study, with even lower optimum growth temperature.

For the direct integration of CNTs into the device process (especially for silicon technology), this is an attractive pathway as the CNTs growth can easily be adjusted to the device process temperature. CNTs can be produced well below 400 °C without any arduous preactivation of the catalyst by a demanding and expensive plasma treatment which is not necessarily compatible with large-scale industrial processes.[16,23] Most of the supports used in this study are common materials in the Si technology as well as active materials for energy conversion and storage. Thus, using the oxidative dehydrogenation reaction of C_2H_2 with CO_2, CNTs can directly be grown on active materials, like V_2O_5, Bi_2O_3, TiO_2, to prepare novel intimate CNT/oxide hybrid systems. Such hybrid materials can provide many advantages over existing materials for batteries, fuel cells, and photovoltaic technologies with the active role of CNTs to assist at the charge extraction and injection from the active materials as well as at the charge transport toward the collecting electrodes.

Our growth experiments have also been extended to support materials with various morphologies. These materials have low melting temperature or poor chemical stability. Therefore, the growth of CNTs is rather difficult when they are used as support under traditional acetylene decomposition conditions. Using the oxidative dehydrogenation reaction of C_2H_2 with CO_2, CNTs have successfully been grown on Cu mesh (Figure 5A,B), cloth made of carbon fibers (Figure 5C,D), and the rim of glass Pasteur pipet (Figure 5E,F). The three supports were previously coated with a 5 nm Fe catalyst film. These new CNT-decorated materials have the potential to make inroads into current applications like highly sensitive conductive glass electrodes, and CNT-coated C fiber composites for sensors, reinforcement, and smart textile applications. The oxidative dehydrogenation reaction of C_2H_2 with CO_2 opens the door to CNT growth at low temperature over metallic particle supported by graphene without the need of NH_3 plasma yielding very likely damages to graphene materials.[24] Growing CNTs directly on Cu is a major breakthrough to build new generation interconnects for CMOS devices. Up to now, the growth of CNTs on a metal substrate was rather poor and/or showed high contact resistance and poor adhesion. Therefore, a CNT via structure was frequently realized by using a Ta barrier layer and a TiN contact layer between the Cu lines and the catalyst for the CNT growth.[25] Alternatively a vertically aligned CNT array was transferred onto a metal substrate using eutectic Sn/Pb, Sn/Au, or Sn/Ag solders.[26,27] Applying the oxidative dehydrogenation reaction of C_2H_2 with CO_2, the major obstacles of growing CNTs directly onto Cu can be overcome: (1) due to the highly enhanced catalyst activity, the chemical interaction between Cu and the metal catalyst is strongly limited leading to high density of CNTs; (2) the CNTs show excellent mechanical and electrical contact with the metal substrate. The resistance of the CNT mat grown directly on Cu was measured using a four-point probe setup (see Support-

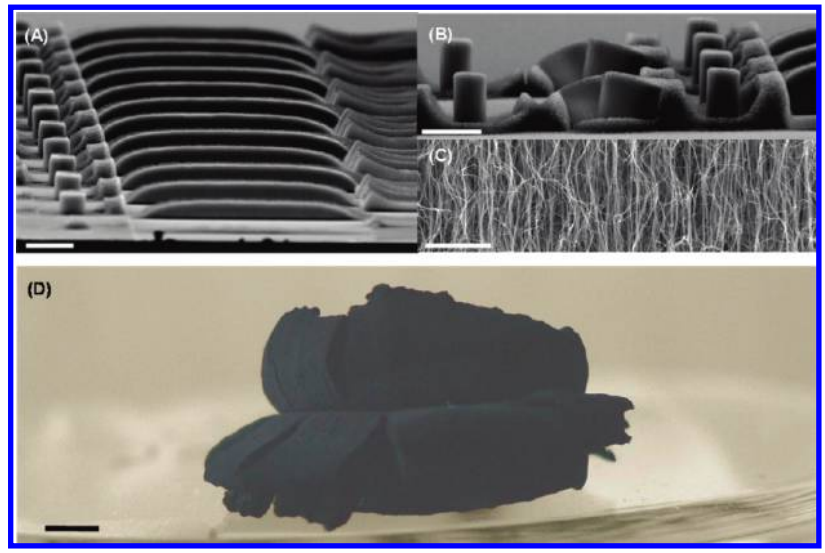

Figure 6. Carbon nanotubes were grown on a Fe film, patterned by e-beam lithography on a Si wafer (scale bar is (A, B) 20 μm and (C) 1 μm). (D) Picture of a 4 mm tall CNTs mat produced on a pellet of Fe_2Co supported by $CaCO_3$ (scale bar is 2 mm).

ing Information). Despite further optimization being required for improving CNTs alignment, the contact resistance measured over a length of 0.25 mm was found to be around 1 Ω/mm^2 suggesting good electrical contact between CNTs and the Cu substrate.

Figure 6 panels A−C illustrate large-scale organized CNT-structures obtained on patterned Fe catalyst on SiO_2-coated Si wafer. A high density of CNTs grows vertically aligned from the substrate surface (Figure 6C). Structures with a height up to 20 μm have been produced. The shape of the structures can be controlled by the standard lithographic patterning of the catalyst on the substrate. Arbitrary shape structures, like pillars and sheets can easily be produced (Figure 6A,B). The highest ordered structures of CNTs have been obtained on the pellet of $Fe_2Co/CaCO_3$ (Figure 6D), with a carpet height of 4 mm. In this case the growth rate is 130 $\mu m \cdot min^{-1}$, being as high as the one obtained by the water-assisted process.[28]

The robustness of the low temperature oxidative dehydrogenation process can be illustrated by the growth of CNTs on everyday objects. We have successfully grown CNTs on one euro cent coin (Figure 7A,B) demonstrating that complex bronze alloys can be used as metallic substrates. Similarly, aluminum cooking foil has also been used successfully as substrate (Figure 7C,D) and remains unaltered under the growth conditions. Actually, growth temperature can be lowered to such an extent that CNTs can also be grown on organic-based materials. We performed the CNT growth at 400 °C for 15 min by coating the tip of a wooden toothpick (Figure 7E,F) with Fe nanoparticles. At the end of the growth process, the core of the toothpick remained intact while the sur-

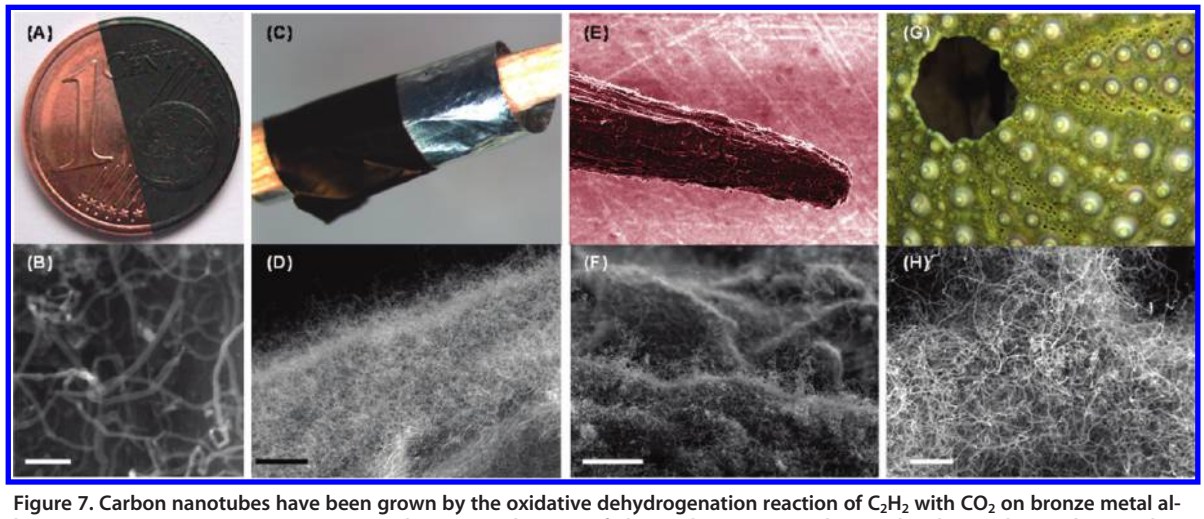

Figure 7. Carbon nanotubes have been grown by the oxidative dehydrogenation reaction of C_2H_2 with CO_2 on bronze metal alloys composing one euro cent coins (A and B), on an aluminum foil (C and D), on a wooden toothpick (E and F), and on a calcite sea urchin shell (G and H). All these supports were decorated with 5 nm Fe film prior to CNT growth by the oxidative dehydrogenation reaction. Scale bars are (B) 200 nm, (D) 5 μm, and (F and H) 2 μm.

face was entirely coated with CNTs. A sea urchin shell coated with metallic nanoparticles can also be used for CNTs growth (Figure 7G,H). Sea shells consist of calcite, which is a sedimentary rock being the third most common constituent of the earth's crust. Indeed, calcite is a highly efficient support material since about 85% of acetylene is transformed into CNTs during the reaction.[29,30] This shows that CNTs can be grown by the oxidative dehydrogenation reaction of C_2H_2 with CO_2 on natural minerals allowing low cost and high yield production of CNTs. Moreover, calcite is the primary ingredient in cement and therefore provides the possibility to develop novel CNT-based materials for construction.

In conclusion, we have reported a simple growth process of CNTs by chemical vapor deposition which is based on the oxidative dehydrogenation reaction of C_2H_2 with CO_2. We have identified two overall chemical mechanisms along which the reaction proceeds which are superior to the reaction based on the traditional thermal decomposition of acetylene. From the technological point of view, the process addresses the issues of the direct integration of CNTs since the growth temperature can be reduced below 400 °C. Moreover, the growth process is highly versatile. Large quantity of CNTs can be grown on various materials which have been unfavorable with the standard growth methods. Consequently, the CNTs synthetic approach based on the oxidative dehydrogenation reaction of C_2H_2 with CO_2 will facilitate the integration of CNTs into numerous applications.

EXPERIMENTAL DETAILS

Catalyst Preparation. Powdered catalyst preparation is performed by the coprecipitation of Fe and Co salts on the surface of support particles. In a typical catalyst preparation process, Fe nitrate and Co nitrate are dissolved in distilled water. Fe/Co ratio is fixed to 2, that ratio being the composition stoichiometry of the most active catalyst in the Fe−Co system.[29−31] Then, support particles are dispersed in the solution. The slurry is kept under vigorous stirring while coprecipitation of Fe and Co salts is induced by the addition to the slurry of a weak base like ammoniac or by water evaporation.

Patterned catalyst deposition on Si growth is performed by e-beam lithography. Fe was deposited by e-beam evaporation. Fe is deposited on the glass Pasteur pipet, carbon textile, euro cent coin, toothpick, aluminum foil, sea urchin shell by thermal evaporation.

Carbon Nanotubes Growth. The growth of carbon nanotubes was performed in a quartz tube furnace at ambient pressure. In a typical growth experiment,[29−31] the catalyst (either powder or deposited on a substrate) is placed in the quartz tube while Ar is introduced at 45 L/h. After 10 min cleaning, a mixture of C_2H_2 and CO_2 (with a 1:1 stoichiometry) is fluxed in the furnace for 15−30 min. Then the reaction chamber is cleaned with Ar for 10 min.

Acknowledgment. We thank the Centre Interdisciplinaire de Microscopie Electronique (CIME) for access to electron microscopes and technical support and D. Acquaviva and A. Arun for preparing patterned catalysts. We thank R. Gaál for the contact resistance measurements. This work was financially supported by the CABTURES project funded by Nano-Tera.ch. M.M. thanks the Swiss National Science Foundation for Grant NSF 121814. The work done by J.C. Andresen and R. Smajda was funded by the European projects VIACARBON (ICT-2007 8.1-216668) and MULTIPLAT (NMP4-SL-2009-228943).

Supporting Information Available: Figures showing the XRD diffractograms of the non-oxide substrates after CNTs growth by the dehydrogenation of acetylene, Raman spectra of CNTs produced over oxide and non -oxide support, the thermodynamic data of the dehydrogenation reactions, SEM micrographs of CNTs produced when Nb_2O_5, carbon fibers, and glass are used as catalyst support. This material is available free of charge *via* the Internet at http://pubs.acs.org.

REFERENCES AND NOTES

1. Harutyunyan, A. R. The Catalyst for Growing Single-Walled Carbon Nanotubes by Catalytic Chemical Vapor Deposition Method. *J. Nanosci. Nanotechnol.* **2009**, *9*, 2480–2495.
2. Dupuis, A. C. The Catalyst in the CCVD of Carbon Nanotubes— A Review. *Prog. Mater. Sci.* **2005**, *50*, 929–961.
3. Joselevich, E.; Dai, H.;, Liu, J.; Hata, K.; Windle, A.H. *Carbon Nanotube Synthesis and Organization*; Jorio, A., Dresselhaus, G., Dresselhaus, M S., Eds.; Topics in Applied Physics, Vol. 111; Springer-Verlag: Berlin, 2008; p 101.
4. de los Arcos, T.; Garnier, M. G.; Seo, J. W.; Oelhafen, P.; Thommen, V.; Mathys, D. The Influence of Catalyst Chemical State and Morphology on Carbon Nanotube Growth. *J. Phys. Chem. B* **2004**, *108*, 7728–7734.
5. Mattevi, C.; Wirth, C. T.; Hofmann, S.; Blume, R.; Cantoro, M.; Ducati, C.; Cepek, C.; Knop-Gericke, A. A.; Milne, S.; Castellarin-Cudia, C.; *et al. In-Situ* X-ray Photoelectron Spectroscopy Study of Catalyst-Support Interactions and Growth of Carbon Nanotube Forests. *J. Phys. Chem. C* **2008**, *112*, 12207–12213.
6. Vander Wal, R. L.; Ticich, T. M.; Curtis, V. E. Substrate-Support Interactions in Metal-Catalyzed Carbon Nanofibre Growth. *Carbon* **2001**, *39*, 2277–2289.
7. de los Arcos, T.; Vonau, F.; Garnier, M. G.; Thommen, V.; Boyen, H. G.; Oelhafen, P.; Duggelin, M.; Mathis, D.; Guggenheim, R. Influence of Iron−Silicon Interaction on the Growth of Carbon Nanotubes Produced by Chemical Vapour Deposition. *Appl. Phys. Lett.* **2002**, *80*, 2383–2385.
8. Nessim, G. D.; Seita, M.; O'Brien, K. P.; John Hart, A.; Bonaparte, R. K.; Mitchell, R. R.; Thompson, C. V. Low Temperature Synthesis of Vertically Aligned Carbon Nanotubes with Electrical Contact to Metallic Substrates Enabled by Thermal Decomposition of the Carbon Feedstock. *Nano Lett.* **2009**, *9*, 3398–3405.
9. Hata, K.; Futaba, D. N.; Mizumo, K.; Namai, T.; Yumura, M.; Iijima, S. Water-Assisted Highly Efficient Synthesis of Impurity-free Single-Walled Carbon Nanotubes. *Science* **2004**, *306*, 1362–1364.
10. Zhang, G.; Mann, D.; Zhang, L.; Javey, A.; Li, Y.; Yenilmez, E.; Wang, Q.; McVittie, J. P.; Nishi, Y.; Gibbons, J.; Dai, H. J. Ultra-High-Yield Growth of Vertical Single-Walled Carbon Nanotubes: Hidden Roles of Hydrogen and Oxygen. *Proc. Natl. Acad. Sci. U.S.A.* **2005**, *102*, 16141–16145.
11. Nasibulin, A. G.; Brown, D. P.; Queipo, P.; Gonzalez, D.; Jiang, H.; Kauppinen, E. I. An Essential Role of CO_2 and H_2O During Single-Walled CNT Synthesis From Carbon Monoxide. *Chem. Phys. Let.* **2006**, *417*, 179–184.
12. Pint, C. L.; Pheasant, S. T.; Nicholas, A.; Parra-Vasquez, G.; Horton, C.; Xu, Y.; Hauge, R. H. Investigation of Optimal Parameters for Oxide-Assisted Growth of Vertically Aligned Single-Walled Carbon Nanotubes. *J. Phys. Chem. C* **2009**, *113*, 4125–4133.

13. Chakrabarti, S.; Kume, H.; Pan, L. J.; Nagasaka, T.; Nakayama, Y. Number of Walls Controlled Synthesis of Millimetre-Long Vertically Aligned Brushlike Carbon Nanotubes. *J. Phys. Chem. C* **2007**, *111*, 1929–1934.
14. Hasegawa, K.; Noda, S.; Sugime, H.; Kakehi, K.; Maruyama, S.; Yamaguchi, Y. Growth Window and Possible Mechanism of Millimetre-Thick Single-Walled Carbon Nanotube Forests. *J. Nanosci. Nanotechnol.* **2008**, *8*, 6123–6128.
15. Amama, P. B.; Pint, C. L.; McJilton, L.; Kim, S. M.; Stach, E. A.; Murray, P. T.; Hauge, R. H.; Maruyama, B. Role of Water in Super Growth of Single-Walled Carbon Nanotube Carpets. *Nano Lett.* **2009**, *9*, 44–49.
16. Lee, D. H.; Lee, W. J.; Kim, S. O. Highly Efficient Vertical Growth of Wall-Number-Selected, *N*-Doped Carbon Nanotube Arrays. *Nano Lett.* **2009**, *9*, 1427–1432.
17. Wang, S.; Zhu, Z. H. Catalytic Conversion of Alkanes to Olefins by Carbon Dioxide Oxidative Dehydrogenation—A Review. *Energy Fuels* **2004**, *18*, 1126–1139.
18. The ratios are calculated from the mass of CNTs produced, the mass of metal nanoparticles, and the mass of support introduced in the reactor.
19. Magrez, A.; Seo, J. W.; Kuznetsov, V. L.; Forró, L. Evidence of an Equimolar $C_2H_2-CO_2$ Reaction in the Synthesis of Carbon Nanotubes. *Angew. Chem., Int. Ed.* **2007**, *46*, 441–444.
20. Jose, R.; Thavasi, V.; Ramakrishna, S. Metal Oxides for Dye-Sensitized Solar Cells. *J. Am. Ceram. Soc.* **2009**, *92*, 289–301.
21. Freund, H. J.; Roberts, M. W. Surface Chemistry of Carbon Dioxide. *Surf. Sci. Rep.* **1996**, *25*, 225–273.
22. Rummeli, M. H.; Schaffel, F.; Bachmatiuk, A.; Adebimpe, D.; Trotter, G.; Borrnert, F.; Scott, A.; Coric, E.; Sparing, M.; Rellinghaus, B.; McCormick, P. G.; Cuniberti, G.; Knupfer, M.; Schultz, L.; Buchner, B. Investigating the Outskirts of Fe and Co Catalyst Particles in Alumina-Supported Catalytic CVD Carbon Nanotube Growth. *ACS Nano* **2010**, *4*, 1146–1152.
23. Zhong, G.; Iwasaki, T.; Kawarada, H. Semiquantitative Study on the Fabrication of Densely Packed and Vertically Aligned Single-walled Carbon Nanotubes. *Carbon* **2006**, *44*, 2009–2014.
24. Lee, D. H.; Kim, J. E.; Han, T. H.; Hwang, J. W.; Jeon, S.; Choi, S. Y.; Hong, S. H.; Lee, W. J.; Ruoff, R. S.; Kim, S. O. Versatile Carbon Hybrid Films Composed of Vertical Carbon Nanotubes Grown on Mechanically Compliant Graphene Films. *Adv. Mater.* **2010**, *22*, 1247–1252.
25. Awano, Y.; Sato, S.; Kondo, D.; Ohfuti, M.; Kawabata, A.; Nihei, M.; Yokoyama, N. Carbon Nanotube *via* Interconnect Technologies: Size-Classified Catalyst Nanoparticles and Low-Resistance Ohmic Contact Formation. *Phys. Status Solidi A* **2006**, *203*, 3611–3616.
26. Kumar, A.; Pushparaj, V. L.; Kar, S.; Nalamasu, O.; Ajayan, P. M. Contact Transfer of Aligned Carbon Nanotube Arrays onto Conducting Substrates. *Appl. Phys. Lett.* **2006**, *89*, 163120.
27. Zhu, L. B.; Sun, Y. Y.; Hess, D. W.; Wong, C. P. Well-Aligned Open-Ended Carbon Nanotube Architectures: An Approach for Device Assembly. *Nano Lett.* **2006**, *6*, 243–247.
28. Futaba, D. N.; Hata, K.; Yamada, T.; Mizumo, K.; Yumura, M.; Iijima, S. Kinetics of Water-Assisted Single-Walled Carbon Nanotube Synthesis Revealed by a Time-Evolution Analysis. *Phys. Rev. Lett.* **2005**, *95*, 056104.
29. Magrez, A.; Seo, J. W.; Mikó, Cs.; Hernadi, K.; Forró, L. Growth of Carbon Nanotubes with Alkaline Earth Carbonate as Support. *J. Phys. Chem. B* **2005**, *109*, 10087–10091.
30. Mionic, M.; Alexander, D. T. L.; Forró, L.; Magrez, A. Influence of the Catalyst Drying Process and Catalyst Support Particle Size on the Carbon Nanotubes Produced by CCVD. *Phys. Status Solidi B* **2008**, *245*, 1915–1918.
31. Smajda, R.; Mionic, M.; Duchamp, M.; Andresen, J. C.; Forró, L.; Magrez, A. Production of High Quality Carbon Nanotubes for Less than $1 per Gram. *Phys. Status Solidi C* **2010**, *7*, 1236–1240.